Comparative Mutant Analysis of Arabidopsis ABCC-Type ABC Transporters: AtMRP2 Contributes to Detoxification, Vacuolar Organic Anion Transport and Chlorophyll Degradation

Annie Frelet-Barrand [1,5], **H. Üner Kolukisaoglu** [2,6], **Sonia Plaza** [3], **Maika Rüffer** [2], **Louis Azevedo** [1], **Stefan Hörtensteiner** [1], **Krasimira Marinova** [1,7], **Barbara Weder** [1], **Burkhard Schulz** [4] and **Markus Klein** [1,*]

[1] Zurich Basel Plant Science Center, University of Zurich, Plant Biology, Zollikerstrasse 107, CH-8008 Zürich, Switzerland
[2] University of Rostock, Institute of Biosciences, Albert-Einstein-Str. 3, D-18059 Rostock, Germany
[3] University of Fribourg, Plant Biology, 3, Albert-Gockel, CH-1700 Fribourg, Switzerland
[4] Purdue University, Horticulture and Landscape Architecture, 625 Agriculture Mall Dr., West Lafayette, IN, 47907-2010, USA

The enormous metabolic plasticity of plants allows detoxification of many harmful compounds that are generated during biosynthetic processes or are present as biotic or abiotic toxins in their environment. Derivatives of toxic compounds such as glutathione conjugates are moved into the central vacuole via ATP-binding cassette (ABC)-type transporters of the multidrug resistance-associated protein (MRP) subfamily. The Arabidopsis genome contains 15 *AtMRP* isogenes, four of which (*AtMRP1*, *2*, *11* and *12*) cluster together in one of two major phylogenetic clades. We isolated T-DNA knockout alleles in all four highly homologous *AtMRP* genes of this clade and subjected them to physiological analysis to assess the function of each *AtMRP* of this group. None of the single *atmrp* mutants displayed visible phenotypes under control conditions. In spite of the fact that AtMRP1 and AtMRP2 had been described as efficient ATP-dependent organic anion transporters in heterologous expression experiments, the contribution of three of the *AtMRP* genes (*1*, *11* and *12*) to detoxification is marginal. Only knockouts in *AtMRP2* exhibited a reduced sensitivity towards 1-chloro-2,4-dinitrobenzene, but not towards other herbicides. *AtMRP2* but not *AtMRP1*, *11* and *12* is involved in chlorophyll degradation since ethylene-treated rosettes of *atmrp2* showed reduced senescence, and *AtMRP2* expression is induced during senescence. This suggests that AtMRP2 is involved in vacuolar transport of chlorophyll catabolites. Vacuolar uptake studies demonstrated that transport of typical MRP substrates was reduced in *atmrp2*. We conclude that within clade I, only *AtMRP2* contributes significantly to overall organic anion pump activity in vivo.

Keywords: *Arabidopsis thaliana* — Gene family — Herbicide resistance — Organic anion transport — Senescence — T-DNA knockout.

Abbreviations: ABC, ATP-binding cassette transporter; ABRC, *Arabidopsis* Biological Resource Center; *Bn*-NCC-1, *Brassica napus* non-fluorescent chlorophyll catabolite 1; BPT1, bile pigment transporter 1; BSA, bovine serum albumin; CDNB, 1-chloro-2,4-dinitrobenzene; CFTR, cystic fibrosis transmembrane conductance regulator; DNB, dinitrobenzene; DTT, dithiothreitol; $E_2$17G, 17β-estradiol 17-(β-D-glucuronide); GFP, green fluorescent protein; GS, glutathione; GS-X, glutathione conjugate; GUS, β-glucuronidase; LTC4, leukotriene C4; NASC, Nottingham Arabidopsis Stock Center; MRP, (ABCC) multidrug resistance-associated protein; NBD, nucleotide-binding domain; ORF, open reading frame; PAR, photosynthetically active radiation; PGP, P-glycoprotein; RT–PCR, reverse transcription–PCR; TMD, transmembrane domain; TWD1, twisted dwarf 1; UTR, untranslated region; YCF1, Yeast cadmium factor 1.

Introduction

The ATP-binding cassette (ABC) protein superfamily is one of the largest protein families known (Henikoff et al. 1997) and its members are found in all organisms investigated. In most cases, eukaryotic ABC transporters mediate the transport of structurally diverse substrates from the cytosol towards extracytosolic compartments including the extracellular space or the central vacuole by directly utilizing ATP hydrolysis to energize this process. As in every good family, notable exceptions to the rule exist. These include ABC proteins lacking a clear transport function such as the cystic fibrosis transmembrane conductance regulator (CFTR) responsible for cystic fibrosis which acts as a chloride channel, and a P-glycoprotein from *Coptis japonica* which is involved in alkaloid uptake rather than export, thus transporting in the 'wrong' direction (Shitan et al. 2003).

[5] Present address: Laboratoire de Physiologie Cellulaire Végétale, iRTSV, CNRS (UMR 5168)/UJF/INRA/CEA, F-38054 Grenoble cedex 9, France.
[6] Present address: University of Rostock, Center for Life Science Automation (celisca), Fiedrich-Barnewitz-Str. 8, D-18119 Rostock, Germany.
[7] Present address: University Hospital Zurich, Clinical Pharmacology and Toxicology, Department of Internal Medicine, Ramistrasse 100/SHO2, CH-8091 Zurich, Switzerland.
*Corresponding author: E-mail, markus.klein@botinst.uzh.ch; Fax, +41-1-634-8204.

The initial discovery of directly energized, ATP-dependent vacuolar transport of glutathione conjugates (GS-Xs) appearing during phase II of detoxification as a result of glutathione S-transferase action on activated toxic substances demonstrated the physiological importance of plant ABC transporters as a novel class of vacuolar ATP-driven pumps (Martinoia et al. 1993). Two approaches established that the subclass of multidrug resistance-associated proteins (MRPs) is involved in detoxification processes. First, the identification of further compounds including endogenously produced substances undergoing ATP-dependent vacuolar transport [e.g. chlorophyll catabolites (Hinder et al. 1996), flavonoids (Klein et al. 2000), alkaloids (Sakai et al. 2002), salicylic acid glucoside (Dean and Mills 2004)] demonstrated that ABC transporters have a more general role in elimination of xenobiotic or plant-derived potentially toxic compounds from the cytosol. Secondly, the identification of human MRP1/ABCC1 in a drug-resistant lung cancer cell line (Cole et al. 1992) together with the characterization of members of the MRP subfamily as ATP-driven pumps for GS-Xs and other organic anions (Konig et al. 1999, Leslie et al. 2005) allowed analysis of MRP-related genes in plants and fungi (reviewed by Klein et al. 2006). MRP proteins are so-called full-size ABC transporters consisting of a pseudo-symmetrical repetition of a transmembrane domain (TMD) followed by a cytosolic nucleotide-binding domain (NBD) which contains the highly conserved Walker A and B sequences known to be intimately involved in and required for the ATP hydrolysis reaction and the ABC signature (LSGGQ) spaced in between the Walker motifs. In most cases and in contrast to other full-size ABC transporters, MRPs possess an N-terminal hydrophobic extension resulting in the general TMD0–TMD1–NBD1–TMD2–NBD2 two-dimensional structure (Fig. 1, Frelet and Klein 2006).

In Saccharomyces cerevisiae, yeast cadmium factor1 (Ycf1) and bile pigment transporter1 (Bpt1) are responsible for the total vacuolar ATP-dependent GS-X transport capacity, while Ycf1 at the same time confers cadmium tolerance to yeasts by its action as a vacuolar transporter for bis(glutathionato)cadmium complexes (Szczypka et al. 1994, Li et al. 1996, Tommasini et al. 1996, Li et al. 1997, Klein et al. 2002, Sharma et al. 2002). In Arabidopsis and rice, 15 and 17 MRP genes, respectively, have been identified (Sanchez-Fernandez et al. 2001, Kolukisaoglu et al. 2002, Jasinski et al. 2003, Klein et al. 2006). Phylogenetic analysis of the 15 AtMRP genes divided them into two subclades, with clade I consisting of AtMRP1 (At1g30400), 2 (At2g34660), 11 (At1g30420) and 12 (At1g30410). Members of each subclade exhibit a high degree of conservation of the exon–intron structure, while AtMRP13 does not cluster with both clades and AtMRP15 represents a pseudogene (Kolukisaoglu et al. 2002). In clade I, members share
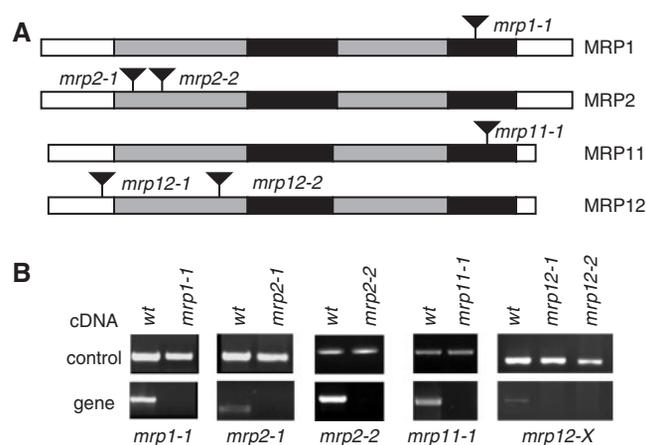
Fig. 1 Structure of the AtMRP1, 2, 11 and 12 genes, position of insert mutants (A) and RT–PCR analysis of clade I AtMRP expression in the wild type and mutants (B). (A) Schematic structures of AtMRP1, 2, 11 and 12 and T-DNA insertion sites. The proposed protein structure for each AtMRP is shown with two transmembrane-spanning domains (TMD1 and 2; gray bars), an N-terminal hydrophobic extension (TMD0, white N-terminal bar) and two nucleotide-binding domains (NBD1 and NBD2; black bars). The insertion sites of T-DNAs in the respective genes (filled triangles) are indicated. (B) RT–PCR analysis verifies the absence of corresponding transcripts in atmrp mutants (mrp1-1, mrp2-1, mrp2-2, mrp11-1, mrp12-1 and mrp12-2) in contrast to the wild-type controls (wt). cDNAs were synthesized from total RNA of mutant and wild-type plants, and transcripts of the 40S ribosomal protein S16-encoding gene (control; upper row) were amplified and detected by RT–PCR. Furthermore, the transcripts of AtMRP1, AtMRP2, AtMRP11 and AtMRP12 (gene, lower row) were amplified from the cDNA of wild-type and corresponding mutant plants as indicated above each lane.

between 68 and 90% amino acid identity, and the AtMRP1, 12 and 11 genes are found on chromosome 1 as a gene cluster in a tandem array and in a head to tail configuration (Kolukisaoglu et al. 2002). The general phylogenetic subclade structure can be found in rice as well. However, clade I in rice consists of only one gene (Klein et al. 2006).

Heterologous expression in yeast and biochemical characterization of five Arabidopsis MRP genes of both subclades demonstrated that they are all capable of catalyzing the MgATP-energized, vanadate-sensitive transport of model GS-Xs such as dinitrobenzene-GS (DNB-GS), suggesting that most of the Arabidopsis MRPs are bona fide transporters for organic anions (for reviews, see Klein et al. 2006, Rea 2007). In spite of their close homology reflected by 87% amino acid identity, AtMRP2 but not AtMRP1 expressed in yeast displayed an enhanced multispecificity and was able to transport Bn-NCC-1, an O-malonylated chlorophyll catabolite of Brassica napus (Liu et al. 2001, Lu et al. 1998). While AtMRP11 and AtMRP12 have not been investigated at all, present evidence using different approaches suggests that

AtMRP1 and AtMRP2 localize to the tonoplast (Liu et al. 2001, Geisler et al. 2004). Interestingly, AtMRP1 and AtMRP2 but not members of clade II physically interact with the C-terminal tetratricopeptide repeat domain of the membrane-bound FKBP-like immunophilin TWD1 (TWISTED DWARF1) which agrees with a modulation of vacuolar metolachlor-GS and 17β-estradiol 17-(β-D-glucuronide) (E$_2$17G) uptake by recombinant TWD1 (Geisler et al. 2004).

In contrast to AtMRP genes of clade II (Gaedeke et al. 2001, Klein et al. 2004), knockout mutants in clade I have not been characterized. Here we report the characterization of individual T-DNA insertion mutants in all clade I AtMRP genes. Only atmrp2 knockout mutants exhibit reduced sensitivity towards the toxic compound 1-chloro-2,4-dinitrobenzene (CDNB). Furthermore, a delay in chlorophyll degradation in atmrp2 plants but not in the other mutants during ethylene-induced senescence suggests that AtMRP2 is involved in the vacuolar transfer of chlorophyll catabolites. Finally, vacuolar uptake of model glutathione and glucuronide conjugates is reduced in atmrp2 mutants. Taken together, we propose that AtMRP2 is partially responsible for vacuolar deposition of GS-Xs and chlorophyll catabolites in vivo, while the other clade I AtMRP genes do not or only marginally contribute to these processes.

Results

### Isolation of T-DNA knockout mutant alleles in AtMRP genes

In an attempt to isolate mutants in AtMRP genes belonging to the clade I subfamily (Kolukisaoglu et al. 2002), a systematic reverse genetic approach was undertaken in collections of T-DNA-transformed Arabidopsis lines obtained from Arabidopsis Stock Centers [Arabidopsis Biological Resource Center (ABRC) at Ohio State, USA, and Nottingham Arabidopsis Stock Centre (NASC), University of Nottingham, UK; U. Kolukisaoglu, A. Möller, A. Zeidler, B. Schulz, unpublished] using 3–5 partially degenerated gene-specific primer pairs per open reading frame (ORF) covering about 11 kb of genomic sequence and including the coding region, and the 5′ and 3′ untranslated region (UTR) of each gene. Degenerated primers were designed to detect T-DNA insertions for several AtMRP genes in the same PCR together with either left- or right-border T-DNA primers performed initially on pools of 1,000 plants. The primers given in Supplementary Table I were successfully used in the isolation and verification of mutant T-DNA alleles.

A mutant allele in AtMRP1 termed atmrp1-1 was isolated from the Feldmann collection of T-DNA mutants (Forsthoefel et al. 1992) initially using the primers mrp1D-a and LB2. Sequencing of the insertion site demonstrated that the insertion had occurred at position +9,009 (+1 marks the

beginning of the ORF of the genomic sequence) in exon 23 of the AtMRP1 sequence, which codes for a region within the cytosolic NBD2 domain (Fig. 1A). A T-DNA mutant in the AtMRP2 gene termed atmrp2-1 was identified in the Tom Jack population of enhancer trap lines in the Col-6/gla1 background (Campisi et al. 1999) initially using the primers mrp12a-s/TJ-LB1. In this case, the T-DNA was found within the AtMRP2 gene at position +1,387 in exon 6, thereby disrupting the characteristic CL3 cytosolic loop interconnecting TMD0 and TMD1. A mutant allele for AtMRP12 termed atmrp12-1 was identified in pools generated from plants of the INRA Versailles collection of T-DNA mutants (Bechtold et al. 1993) with the primer pair MRP11/12-S1/VsLB1. However, in atmrp12-1 we were not able to locate the right border. The T-DNA insertion identified with the left border is at position +846 at the donor site of intron 3. Further mutant alleles were found by database searches in the SALK collection of T-DNA lines (Alonso et al. 2003). Verification of mutations in plants grown from seeds received from the NASC resulted in the identification of atmrp2-2 with the T-DNA insertion at position +3,453 in intron 11 (SALK_127425) and atmrp11-1 with an insertion at position +6,894 in exon 23 (SALK_072784). Finally, a second mutant allele for AtMRP12 termed atmrp12-2 was found in the SALK collection with a T-DNA insertion at position +3,515 in exon 15 (SALK_057394). Sequence analysis performed with PCR products obtained from both borders of the inserted T-DNA demonstrated that the T-DNA insertion resulted in the deletion of 62 and 12 bp of gene sequence in atmrp2-2 and atmrp11-1, respectively, while no deletion could be found for atmrp12-2. Finally, reverse transcription–PCR (RT–PCR) analysis performed on total RNA extracted from aerial parts of soil-grown wild-type and mutant plants proved the absence of the corresponding transcripts in homozygous plants of all described mutants (Fig. 1B).

Toxicity assays

Heterologous expression of AtMRP1 and AtMRP2 in yeast demonstrated that these ABC transporters are able to transport GS-Xs in an ATP-dependent manner (Lu et al. 1997, Lu et al. 1998, Liu et al. 2001). Therefore, it had been argued that both transporters are actively involved in phase III of detoxification ultimately transferring conjugated detoxified compounds into the vacuole. Using our collection of T-DNA mutants for clade I AtMRP genes, we directly tested whether detoxification of different xenobiotic compounds is compromised in single AtMRP knockouts. Null mutants and wild-type plants were germinated in the light on sterile plates containing a logarithmic series of concentrations up to 0.1 mM of the sulfonylurea herbicide primisulfuron, the chloroacetanilide herbicide metolachlor and the triazine derivative atrazine. None of the mutants
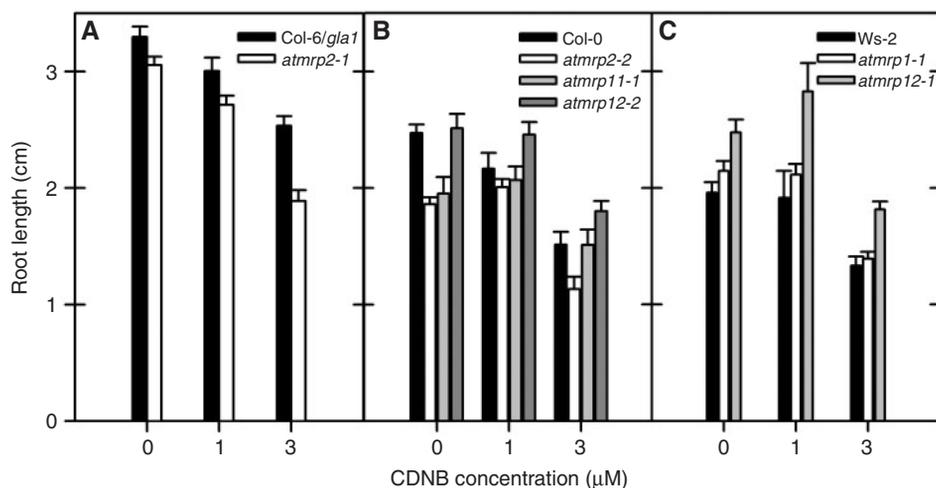
Fig. 2 Mutants in *AtMRP2* but not *atmrp1, 11* and *12* mutants exhibit increased sensitivity towards 1-chloro-2,4-dinitrobenzene (CDNB). Sterile seeds of the indicated *atmrp* mutants and their corresponding wild types were grown on 1/2 MS/1% sucrose agar plates in the absence or presence of CDNB. Depicted is the root length of the mutants grown together with that of their corresponding wild types: (A) *atmrp2-1* (open bar) and Col-6/*gla-1* (black filled bar); (B) *atmrp2-2* (open bar), *atmrp11-1* and *atmrp12-2* (filled, light and dark gray bars, respectively) and Col-0 (black filled bar); (C) *atmrp1-1* (open bar), *atmrp12-1* (filled gray bar) and Ws-2 (black filled bar). The Mann–Whitney test was used to compare root length between mutants and their corresponding wild type. Only *atmrp2* mutants differed significantly from their respective wild type (mean $\pm$ SEM, $P < 0.05$, $n > 20$).

exhibited changes in sensitivity towards any of the herbicides applied as compared with the respective wild types (data not shown). However, under control conditions without any toxic compound added, the *atmrp12-1* but not the *atmrp12-2* allele exhibited a slightly increased root growth, while root growth of *atmrp2-2* and *atmrp11-1* but not of *atmrp2-1* was slightly reduced when compared with the wild type (Fig. 2). In addition to the above-mentioned herbicides, the toxic compound CDNB, a classical substrate of glutathione *S*-transferases (Edwards 1996), was applied. In contrast to herbicide treatments, root growth of both *atmrp2* alleles was affected when plants were treated with 1 and 3 μM CDNB. In the presence of 3 μM CDNB, the root length of *atmrp2* mutants was reduced to about 80% of the wild-type root length, and this difference in root growth was significant at the $P < 0.05$ level (Fig. 2A, B). Root growth reduction by CDNB in all other *atmrp* mutants was indistinguishable from that of the corresponding wild types (Fig. 2B, C). In contrast, submicromolar concentrations of CDNB did not result in significant hypersensitivity of the *atmrp2* mutant alleles. CDNB at ≥ 10 μM abolished plant growth in all lines. Therefore, with respect to CDNB, single knockout mutants demonstrated a significant contribution of AtMRP2 to intracellular detoxification in vivo.

AtMRP2 is involved in chlorophyll degradation in vivo

During senescence, chlorophyll catabolites such as the non-fluorescent chlorophyll catabolite *Bn*-NCC-1 from *Brassica napus* are ultimately deposited into the vacuole via an ABC transporter (Hinder et al. 1996). Heterologous

expression of *AtMRP2* and the clade II gene *AtMRP3* in yeast demonstrated that these AtMRPs but not AtMRP1 are able to transport *Bn*-NCC-1 in an ATP-dependent manner, suggesting that AtMRPs contribute to chlorophyll catabolism (Lu et al. 1998, Tommasini et al. 1998). Therefore, we investigated whether single knockouts in clade I *AtMRP* genes were affected in chlorophyll degradation and senescence (Fig. 3). Naturally senescing single mutants as well as fully grown excised rosette leaves transferred into permanent darkness did not exhibit any mutant-related phenotypical change in chlorophyll degradation (data not shown). However, when identically grown single plants that did not exhibit any visible signs of senescence in rosette leaves were exposed to 20 p.p.m. ethylene for 2 d, ethylene promoted senescence as judged by leaf yellowing and disappearance of chlorophyll (Fig. 3A). Excised rosette leaves of C_2H_4-treated, 7-week-old single wild-type plants lined up in a developmental series (leaf No. 1 corresponding to the youngest leaf) underwent ethylene-induced senescence as observed by the yellowing of leaf 12–14 onwards depending on the ecotype. In contrast, both *atmrp2* alleles exhibited a mild stay-green phenotype when compared with the corresponding wild-type ecotypes: while leaves Nos. 12–16 and 15–21 of Col-6/*gla-1* and Col-0, respectively, were yellow due to chlorophyll degradation, the corresponding leaves of the *atmrp2-1* and *atmrp2-2* plants were still green or at least much less affected by chlorophyll degradation (Fig. 3A). In order to quantify this effect, total chlorophyll was measured in individual rosette leaves, and the relative

content in C_2H_4-treated vs. untreated control leaves was compared (Fig. 3B). Care was taken to compare corresponding leaves directly within the developmental series by starting with single plants possessing identical numbers of leaves. To calculate the relative content, the chlorophyll content of an individual C_2H_4-treated leaf was divided by the chlorophyll content of the corresponding untreated sample, and the calculated relative content of the first, youngest sampled leaf was set to a value of 1. As can be seen from Fig. 3B, all wild-type ecotypes exhibited a gradual, age-related decrease in relative chlorophyll content upon C_2H_4 exposure. Furthermore, C_2H_4-induced chlorophyll degradation in *atmrp1-1* mutant leaves (Fig. 3B, right panel) as well as in rosette leaves of *atmrp11-1* and *atmrp12-1* (data not shown) proceeded as in the corresponding wild-type plants. Confirming the observation in Fig. 3A, rosette leaves of both T-DNA mutants in *AtMRP2* retained significantly more chlorophyll ($P < 0.05$ for leaves No. 10–20 for *atmrp2-1* and leaves No. 12–20 for *atmrp2-2*) after exposure to C_2H_4 as reflected by a slower decrease in relative chlorophyll content in individual leaves along the series (Fig. 3B, left and middle panel). Although a senescence-associated phenotype was not clearly visible in naturally senescing *atmrp2* mutants, the expression of the *AtMRP2* gene is induced during natural senescence or when senescence is induced by dark incubation of excised rosette leaves (Fig. 3C, D). After 3–9 d in darkness, the *AtMRP2* transcript level was increased in semi-quantitative RT–PCR experiments when compared with the transcript level present in rosette leaves prior to dark treatment. In addition, to investigate the effect of natural senescence on *AtMRP2* expression, leaves possessing only 87 or 54% of the chlorophyll content measured in non-senescent leaves were chosen for RNA isolation. Again, when compared with non-senescing controls, a higher level of *AtMRP2* transcript was detected in leaves undergoing natural senescence (Fig. 3C, D). Taken together, mutant analysis in clade I *AtMRP* genes suggested that *AtMRP2* but not the other genes contributes to chlorophyll degradation probably by the action of AtMRP2 as a vacuolar transporter for chlorophyll catabolites or by an overall alteration of the senescence process. Furthermore, *AtMRP2* is regulated on the transcriptional level during senescence.

A knockout in AtMRP2 results in decreased vacuolar organic anion transport

Only *atmrp2* single mutants exhibited phenotypes characterized by increased sensitivity towards CDNB and delayed chlorophyll degradation which could be interpreted as defects in vacuolar MRP-related transport activities. Mutants in *AtMRP1*, *11* and *12* were indistinguishable from their wild types in all experiments performed. In order to test directly whether a knockout in *AtMRP2* affects

vacuolar transport activities, mesophyll vacuoles were isolated from Col-6/*gla-1* and *atmrp2-1* rosette leaves, and transport experiments were performed using two classical substrates of MRP-type ABC transporters. In yeast expression experiments, it has been demonstrated that AtMRP2 mediates transport of GS-Xs as well as glucuronide conjugates. Col-6 mesophyll vacuoles possessed ATP-dependent transport activities for the organic glucuronide E_217G which appears in the mammalian liver during steroid degradation, as already demonstrated for a variety of mono- and dicotyledonous plants (Table 1; Klein et al. 2006). Efficient inhibition of vacuolar E_217G uptake by vanadate confirmed that transport occurred via an ABC transporter. In contrast, E_217G uptake was significantly reduced to about 70% when vacuoles were isolated from *atmrp2-1* plants ($P < 0.05$). In a second series of uptake experiments, we investigated the transport activity with GS-Xs. Pilot experiments demonstrated that Arabidopsis vacuoles possessed a rather low transport activity when radiolabeled DNB-GS was used as a substrate (data not shown). Therefore, [^{3}H]leukotriene C4 (LTC4) was included in transport experiments. LTC4 is synthesized in bone marrow-derived leukocytes through the conjugation of glutathione to LTA4, and represents a high-affinity substrate for selected human MRP/ABCC transporters (Leier et al. 1994). LTC4 was efficiently taken up into Arabidopsis Col-6 vacuoles in an ATP-dependent and vanadate-sensitive manner (Table 1). As for the glucuronide, LTC4 transport rates were significantly reduced to about 60% of the wild-type uptake activity when experiments were performed with vacuoles isolated from *atmrp2-1* plants ($P < 0.05$). For both substrates, vanadate efficiently inhibited transport into *atmrp2* vacuoles to values seen in the wild type ($P < 0.05$). Previous studies using isolated rye and barley vacuoles and the characterization of transport activities of heterologously expressed *AtMRP2* demonstrated that transport of glucuronides such as E_217G is strongly stimulated by DNB-GS (Klein et al. 1998, Liu et al. 2001). However, glucuronide transport rates into Arabidopsis vacuoles (Col-6 and *atmrp2-1*) were not increased when 0.2 mM DNB-GS was added (Table 1).

AtMRP1 and AtMRP2 promoter–GUS fusions suggest partially differential expression in roots, cotyledons and flowers

RT–PCR analysis of the expression of *AtMRP1* and *AtMRP2* in different tissues revealed that *AtMRP1* is expressed mainly in leaves, roots, flowers and stems, but less in siliques, and that *AtMRP2* is expressed at a lower level in all these organs (Kolukisaoglu et al. 2002). In order to determine the tissue specificity of the expression of these genes in more detail, the upstream transcriptional regulatory region was examined. A 2.5 kb genomic fragment of
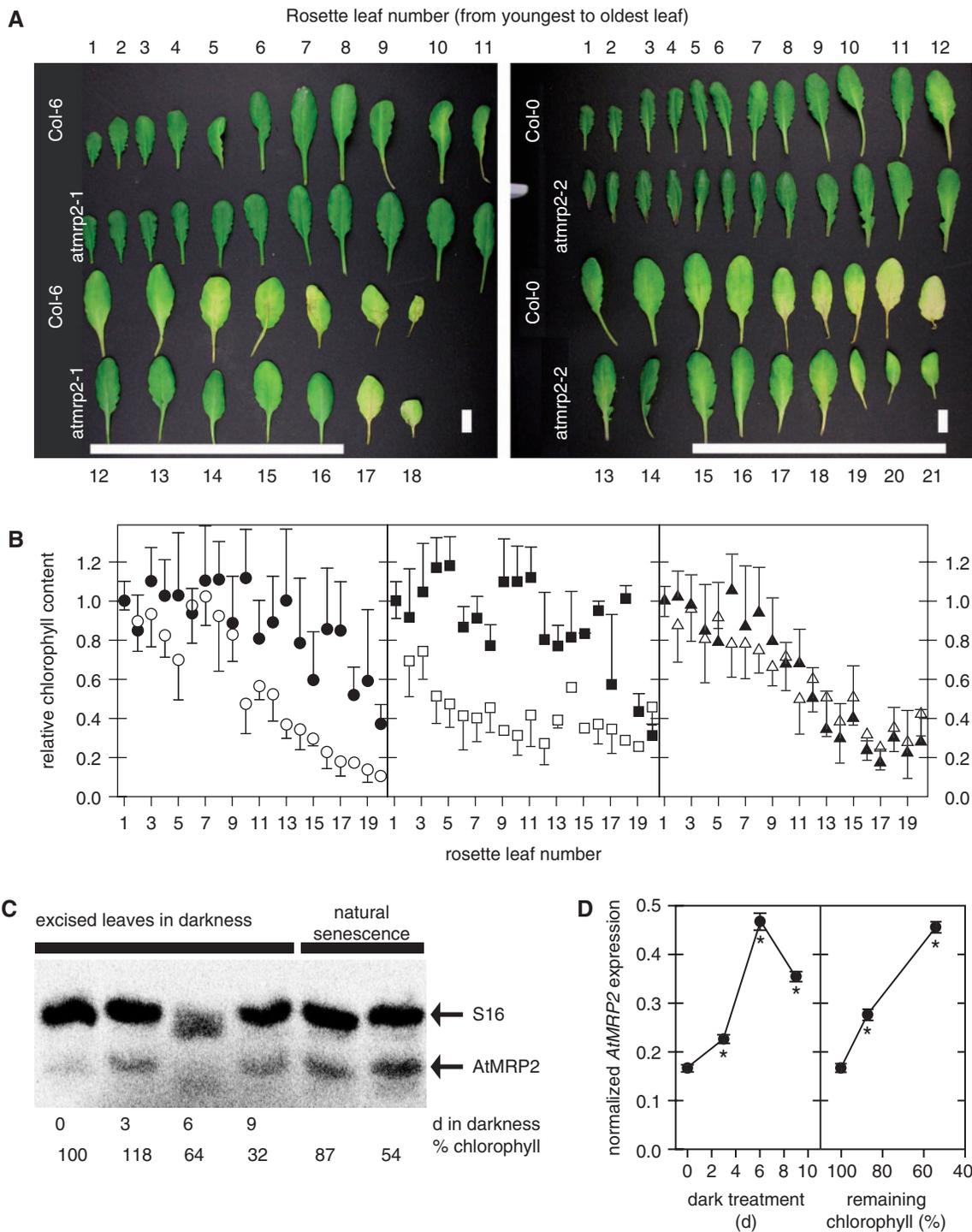
Fig. 3 AtMRP2 affects chlorophyll catabolism. (A, B) *atmrp2* mutants are delayed in chlorophyll degradation. (A) A series of excised rosette leaves of Col-6, *atmrp2-1* (left panel) and Col-0, *atmrp2-2* single plants (right panel) after treatment of intact plants with 20 p.p.m. ethylene for 2 d. Leaves of individual plants were arranged from the youngest (top left) to the oldest leaf (bottom right). The rosette leaf numbers are indicated above and below the panels. The horizontal white bar highlights leaves with a marked difference in chlorophyll degradation when wild-type and *atmrp2* alleles are compared. Vertical white bar = 1 cm. (B) Ethylene-treated *atmrp2* but not *atmrp1* alleles display a stay-green phenotype. All rosette leaves of ethylene-treated and control plants were collected as depicted in (A) and the chlorophyll content of each individual leaf was measured. The chlorophyll content of ethylene-treated leaves was divided by the content measured in untreated leaves of the corresponding position within the rosette. This ratio was set to 1 for the first, youngest leaf, and all other ratios were calculated accordingly. Left panel, Col-6 and *atmrp2-1*; middle panel, Col-0 and *atmrp2-2*; right panel, Ws-2 and *atmrp1-1*.

Table 1 ATP-dependent uptake of [^{3}H]estradiol 17-β-ᴅ-glucuronide (E$_2$17G) or [^{3}H]leukotriene C4 (LTC4) into rosette leaf mesophyll vacuoles isolated from *atmrp2-1* and its corresponding wild type (Col-6/*gla1*) in the presence of MgATP

Line/treatment	Transport into isolated mesophyll vacuoles [pmol × (μl vacuolar volume × min)$^{-1}$]	
	Substrate	
	E$_2$17G	LTC4
Col-6/*gla1*	0.82 ± 0.10 (100%)	308 ± 71 (100%)
Col-6/*gla1* + 1 mM vanadate	0.15 ± 0.03 (18%)	18 ± 6 (6%)
Col-6/*gla1* + 0.2 mM DNB-GS	0.65 ± 0.07 (79%)	n.d.
atmrp2-1	0.55 ± 0.10 (67%)[*]	175 ± 24 (57%)[*]
atmrp2-1 + 1 mM vanadate	0.10 ± 0.05 (12%)[*]	11 ± 5 (3.5%)[*]
atmrp2-1 + 0.2 mM DNB-GS	0.43 ± 0.08 (53%)[*]	n.d.

In the absence of AtMRP2, ATP-dependent organic anion transport rates are reduced to 60–70%. n.d., not determined. The Mann–Whitney test was used to compare transport activity between vacuoles isolated from *atmrp2-1* and Col-6/*gla-1*. When marked with an asterisk, *atmrp2* activities were significantly different from Col-6/*gla-1* (mean ± SD, $P < 0.05$, $n = 5$).

the putative *AtMRP1* and *AtMRP2* promoter regions (Pro$_{AtMRP1}$ and Pro$_{AtMRP2}$) was fused to the *uidA* reporter gene, and β-glucuronidase (GUS) activity was analyzed in sterile-grown seedlings and soil-grown plants at different stages of development (Fig. 4). GUS activity of 4-day-old Pro$_{AtMRP1}$::*GUS* T$_3$ seedlings ($n ≥ 11$ independent homozygous, single insertion transformants) could be detected in all plant parts (Fig. 4A) with the exception of the root tip and the root elongation zone (Fig. 4A3). Interestingly, GUS staining of Pro$_{AtMRP2}$::*GUS* roots was high in the root tip and elongation zone, and decreased towards the hypocotyl (Fig. 4B). GUS activity of Pro$_{AtMRP2}$::*GUS* lines was low in cotyledons, which were strongly stained in the case of Pro$_{AtMRP1}$::*GUS* seedlings, with the highest activity in the vascular bundles (Fig. 4A1, B1). Emerging primary leaves as well as rosette leaves exhibited Pro$_{AtMRP1}$- and Pro$_{AtMRP2}$-driven GUS activity (Fig. 4A2, B2, C, D). Except for the higher activity in vascular bundles, GUS staining appeared rather uniformly distributed in leaves. In flowers, Pro$_{AtMRP1}$::*GUS* activity was high in sepals and towards the stigma (Fig. 4E), while *AtMRP2* expression based on GUS activity was not detectable in this organ (Fig. 4H). Maturing, yellow pods exhibited Pro$_{AtMRP1}$-driven GUS activity in the vascular bundles of the fruit wall, while GUS activity of Pro$_{AtMRP2}$::*GUS* was low in siliques (Fig. 4F, J).

Discussion

A mutant approach allows the dissection of single gene effects in a small redundant transporter subfamily

Due to their sessile lifestyle, plants have evolved an enormous metabolic plasticity as well as mechanisms to detoxify various harmful compounds. One strategy of detoxification is the efficient protection of the cytosol by transfer of conjugated substances into the vacuole, a process which involves MRP-type ABC transporters (Klein et al. 2006). Using a reverse genetic strategy and physiological approaches, we could assign a role for *AtMRP2* within the subclade I of four highly homologous, redundant Arabidopsis MRP transporters. Notably, for ABC transporters, redundancy does not exist solely at the genetic level but also at the level of protein function since many are well known for their broad and overlapping substrate specificities. However, only *atmrp2* mutants exhibited changes in xenobiotic detoxification and chlorophyll degradation, and a reduction in overall vacuolar anionic conjugate transport activity.

Our results demonstrate that none of the four clade I genes encodes the 'major' transporter responsible for herbicide detoxification into the vacuole since we did not observe drastic changes in sensitivities towards different herbicides (Fig. 2). Thus, either a clade II *AtMRP* has the

Fig. 3 Continued

Open symbols, wild types; filled symbols, *atmrp* mutants. A significant difference (Mann–Whitney, $P < 0.05$ and $n = 3–6$, mean ± SD) was obtained between the wild type and *atmrp2* mutants for leaves Nos. 10 and 20 and Nos. 12 and 20 for *atmrp2-1* and *atmrp2-2* alleles, respectively.(C) Semi-quantitative RT–PCR demonstrates that *AtMRP2* expression is slightly increased when either single excised rosette leaves are kept in permanent darkness or soil-grown Arabidopsis plants undergo natural senescence. Autoradiograph of a representative RT–PCR experiment in the presence of [^{33}P]dCTP (22 cycles). Amplification was performed as a multiplex PCR in the presence of an intron-spanning primer pair for *AtMRP2* and a primer pair specific for the 40S ribosomal protein S16 gene (see arrows) using cDNA prepared from total RNA of excised leaf material kept in darkness for a defined period (days in darkness) or exhibiting the indicated loss of chlorophyll during natural senescence given as percentage chlorophyll. (D) Normalized histogram of RT–PCR results ($n = 3$) exhibiting increasing AtMRP2/S16 expression ratios in excised leaves (left panel) or during natural senescence (right panel). Significant differences (Mann–Whitney, $P < 0.05$, mean ± SD) compared with non-senescent controls are indicated by an asterisk.
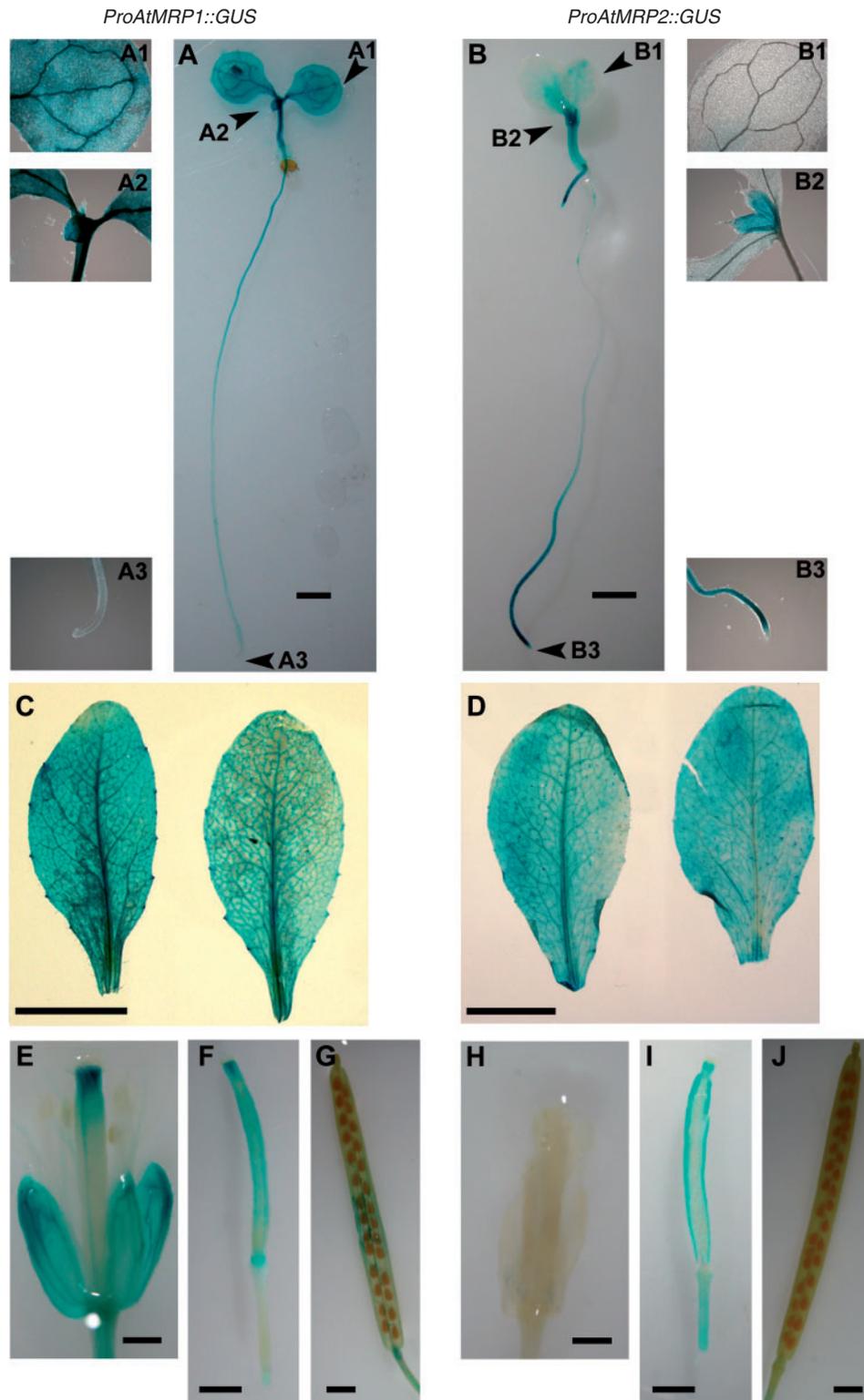
Fig. 4   Analysis of GUS activity in transformed Pro_{AtMRP1}:GUS (A, C, D, E, F, G) and Pro_{AtMRP2}:GUS (B, D, H, I, J) Arabidopsis plants. Depicted are the results of GUS staining analysis performed with 4-day-old sterile grown seedlings (A, B) or the following tissues or plant parts of soil-grown adult plants: rosette leaves (C, D), flowers (E, H), siliques 2 d after pollination (F, I) and mature, yellow siliques (G, J). Small panels (A1–A3; B1–B3) are microscopic pictures of selected plant parts highlighted by arrows in the corresponding binocular images A and B, respectively. A, B, G, J, bar = 1.5 mm; C, D, bar = 10 mm; E, F, H, I, bar = 1 mm.

primary function as a vacuolar conjugate pump for toxic compounds or several *AtMRP* genes act redundantly to achieve this transport function. Alternatively, it could be argued that the importance of vacuolar transfer (phase III of detoxification; Coleman et al. 1997) is overestimated since herbicides undergoing detoxification are already much less harmful upon attachment of hydrophilic molecules such as glucose or glutathione in phase II (Kreuz et al. 1996).

Single-gene knockout mutations reveal that AtMRP2 is involved in chlorophyll degradation during senescence in vivo

Only the *atmrp2* knockout plants exhibited phenotypes related to initially proposed AtMRP functions (Rea et al. 1998): a weakly increased sensitivity towards CDNB (Fig. 2), a delay in chlorophyll degradation during ethylene-induced senescence (Fig. 3) and a partial loss of vacuolar ATP-dependent, vanadate-sensitive organic anion transport activity (Table 1). Thus, the analysis of single-gene mutants partially confirms the analysis of kinetic properties of AtMRP1 and AtMRP2 expressed in yeast: AtMRP2 but not AtMRP1 was able to transport the chlorophyll catabolite *Bn*-NCC-1, and the overall organic anion transport capacity was estimated to be greater for AtMRP2 than for AtMRP1 (Lu et al. 1998, Liu et al. 2001).

During senescence, the transcript level of *AtMRP2* increases when Arabidopsis plants undergo natural senescence or when chlorophyll degradation is induced by placing rosette leaves into the dark (Fig. 3C, D). This result is confirmed by comparative transcriptome data demonstrating that *AtMRP2* expression was induced up to 8.7-fold when Arabidopsis leaves undergo natural senescence. In contrast, induction of *AtMRP1* expression was weaker during senescence, resulting in a factor of 2.7 (Buchanan-Wollaston et al. 2005). We did not observe a senescence-related phenotype in our collection of single-gene mutants in clade I *AtMRP* genes when plants underwent natural senescence. However, when senescence was induced by ethylene, rosette leaves of *atmrp2* mutants displayed a stay-green phenotype that was visible in developmentally 'older' leaves and could be quantified as a lack of ethylene-induced chlorophyll decomposition in *atmrp2* leaves (Fig. 3A, B). In contrast, *atmrp1*, *11* and *12* mutants were indistinguishable from their corresponding wild types, suggesting that *AtMRP2* is functionally unique with respect to this phenotype or the contribution of other clade I transporters is less pronounced.

In order to rule out whether *AtMRP2* expression is under direct control of ethylene, we mined the available 22k Affymetrix Arabidopsis transcriptome data sets using Genevestigator (Zimmermann et al. 2004). Neither *AtMRP1* nor *AtMRP2* expression is strongly affected by short-term treatments with ethylene or ethylene biosynthesis inhibitors (data not shown). *AtMRP11* and *AtMRP12*

cross-hybridize on the Affymetrix chips and therefore cannot be resolved. Co-expression analysis performed with the ATTED-II *trans*-factor and *cis*-element prediction database (Obayashi et al. 2007) did not reveal any indication that *AtMRP2* expression is correlated to the expression of ethylene biosynthesis or signaling genes. We interpret these results as an indication that the phenotype observed in *atmrp2* mutants is senescence related rather than ethylene induced, which is in accordance with our expression data. Thus, in our experiment (Fig. 3) ethylene only accelerates senescence whereas it most probably does not directly affect the function of AtMRP2. Taken together, it can be hypothesized that AtMRP2 acts as a vacuolar transporter for chlorophyll catabolites whereas mutant plants undergoing senescence are partially impaired in catabolite deposition into the vacuole. As a consequence, *atmrp2* mutants slow down chlorophyll degradation by a feedback mechanism in order to avoid the hyperaccumulation of potentially photo-toxic chlorophyll breakdown intermediates.

Reduced vacuolar transport activities in the atmrp2-1 mutant

The ATP-dependent, vanadate-sensitive vacuolar transport activities for the glutathione conjugate LTC4 and the glucuronide $E_2$17G—two model substrates for MRP/ABCC-type transporters—were reduced to 60 and 70%, respectively, when mesophyll vacuoles isolated from *atmrp2-1* were compared with the corresponding wild type vacuoles (Table 1). Thus, within a gene family of 15 genes, AtMRP2 clearly contributes to vacuolar transport of organic anions. This result is in accordance with studies comparing the kinetic properties of AtMRP1 and AtMRP2 in yeast vesicles (Lu et al. 1997, Lu et al. 1998, Liu et al. 2001). Transport of DNB-GS and a metolachlor-GS conjugate formed with the chloroacetanilide herbicide metolachlor occurred with comparable affinities (K_m values $\sim$70 μM) while the K_m for oxidized glutathione was 3-fold higher for AtMRP1 than for AtMRP2. The V_{max} was clearly greater for AtMRP2 than for AtMRP1 for all substrates, suggesting that AtMRP2 possessed a higher catalytic capacity when compared with AtMRP1. Furthermore, AtMRP2 expressed in yeast was found to be unique in the sense that the application of combinations of transport substrates resulted in a complex cross-regulation of individual transport activities (Liu et al. 2001). These authors suggested that AtMRP2 possesses multiple binding sites interconnecting three or four semi-autonomous transport pathways for structurally distinct substrates. Interestingly, Arabidopsis mesophyll vacuoles did not display indications of cross-stimulation of organic anion transport since transport of $E_2$17G was not stimulated by the GS-conjugate DNB-GS in our experiments. This result contradicts earlier transport experiments performed with rye and barley vacuoles where glucuronide transport was

strongly stimulated by GS-Xs (Klein et al. 1998). One possible hypothesis explaining cross-stimulation of ectopically expressed *AtMRP2* but absence of stimulation on Arabidopsis vacuoles is that Arabidopsis vacuoles contain an unknown component that negatively controls GS-X stimulation of glucuronide transport which is absent or less stringently acting in cereals. Geisler et al. (2004) have recently shown that the membrane-bound immunophilin TWD1, which interacts with AtMRP1 and 2, affects organic anion transport in Arabidopsis vacuoles. It is tempting to speculate that TWD1 also inhibits the modulation of MRP-related transport activities in Arabidopsis, e.g. by glutathione and its derivatives.

Expression of AtMRP1 and AtMRP2 is partially overlapping in leaves and the hypocotyl, but distinct in roots, cotyledons and flowers

According to a preliminary RT–PCR analysis, all clade I *AtMRP* genes are expressed in all tissues and plant parts investigated (Kolukisaoglu et al. 2002). Promoter–GUS fusions with the promoters of *AtMRP1* and *AtMRP2* studied here are active in different tissues and to different extents, suggesting diversity at the level of transcript abundance. In seedlings, both promoters produce GUS activity in the hypocotyl, while the staining pattern of roots suggests that *AtMRP2* is more abundant in the developing and elongating zones of the root whereas the promoter of *AtMRP1* is more active in the basal root parts (Fig. 4). With regard to the increased sensitivity of sterile-grown *atmrp2* alleles towards CDNB which primarily resulted in a reduction of root growth (Fig. 2), the question arises as to whether toxic effects caused by this compound are more severe in *atmrp2* mutants because cell division and root elongation are more directly affected in the absence of *AtMRP2* while lack of *AtMRP1* is less drastic because its presence in these tissues is reduced anyway when compared with *AtMRP2*. In contrast, the GUS staining pattern in rosette leaves is comparable for both genes, although a delay in leaf senescence (Fig. 3) and a lower transport activity of mesophyll vacuoles (Table 1) was specific for *atmrp2* mutants. This latter observation suggests that differences in the catalytic activity and substrate specificity of the clade I *AtMRP* genes contribute significantly to the in vivo function of individual transporters within this gene family.

With respect to the functions of clade I *MRP* genes, it will be interesting to investigate the phenotype(s) of plants lacking all genes. In Arabidopsis, genetic crosses of single-gene knockouts with the quadruple knockout are hampered by the fact that *AtMRP1*, *12* and *11* are arranged as tandem duplications on chromosome 1. In order to overcome this problem, a knockout rice plant lacking *OsMRP1* could be studied. *OsMRP1* is the only *MRP* gene exhibiting high homology to the *Arabidopsis* clade I members (Jasinski et al.

2003, Klein et al. 2006). Thus, investigation of *OsMRP1* will be helpful to understand the conservation of physiological functions of clade I MRPs across different species.

Materials and Methods

Chemicals

Unless otherwise stated, all chemicals were from Sigma (Buchs, Switzerland). MS medium (Murashige and Skoog 1962) was from Duchefa (Haarlem, The Netherlands; No. M0233). $[6,7-^3H(N)]E_217G$ (specific activity $45\,Ci\,mmol^{-1}$) and $[14,15,19,20-^3H(N)]LTC4$ ($158\,Ci\,mmol^{-1}$) were obtained from PerkinElmer Life Sciences Inc. (Boston, MD, USA). All herbicides were a kind gift of Dr. Klaus Kreuz (BASF AG, Ludwigshafen, Germany), and herbicides and CDNB were dissolved as stocks of 10 mM in dimethylformamide and ethanol, respectively.

Plant culture, senescence induction and herbicide toxicity assay

If not stated otherwise, *Arabidopsis thaliana* wild types, mutants and transgenic lines were grown from stratified (48 h at 4°C) seeds on soil in phytotrons with a 8 h light period (21°C; 70% relative humidity; $200\,\mu mol\,m^{-2}\,s^{-1}$ PAR) and were watered twice a week. Upon germination on soil for 3 weeks, single plants were transferred into new pots which were kept at 8 h of light for another 3 weeks before use. For vacuole isolations, 3-week-old single plants were maintained in a growth chamber with 10 h light ($150\,\mu mol\,m^{-2}\,s^{-1}$ PAR; 21°C; 70% relative humidity) for an additional 4 weeks. For the analysis of *AtMRP2* expression in senescing rosette plants, plants grown for 8 weeks under short day conditions were used. Senescence was induced by placing individual fully expanded rosette leaves in a Petri dish with wet filter paper in darkness for 0, 3, 6 and 9 d (dark-induced senescence). Alternatively, attached leaves that had already started to senesce (developmental senescence), containing approximately 87 and 54% of the original chlorophyll content, were taken for RNA isolation. For the phenotypical investigation of chlorophyll degradation during ethylene-induced senescence, 7-week-old single plants, all possessing an identical number (<20) of rosette leaves, were transferred into closed glass containers and treated with 0 (control) or 20 p.p.m. C_2H_4 released from ethephon for 2 d.

All antibiotic resistance and segregation assays as well as herbicide tolerance tests were performed with bleach-sterilized, stratified seeds germinated on solid half-strength MS medium containing 1% (w/v) sucrose. Plates were placed in a growth room in a vertical position with light from the top (16 h), and root length was scored after 1 week. For all phenotypical and physiological investigations, care was taken to use several independent wild-type and mutant seed batches that were obtained from identically treated plants.

Isolation of mutant alleles

A collection of about 60,000 T-DNA insertion lines available through the Arabidopsis Stock Centers at Ohio State (ABRC) and the University of Nottingham (NASC) were screened for *AtMRP1*, *2* and *12* knockout alleles. To screen the entire coding region of these genes, a set of partially degenerated primers was designed (see Supplementary Table I). These primers were used in combination with T-DNA-derived border primers in PCRs with DNA from T-DNA-transformed plants arranged in pools of 1,000 plants. Subsequent rounds of re-amplification of PCR products and generation of hybridization probes were performed with nested

PCR primers to avoid cross-reactions with the primary PCR primer sequences.

T-DNA insertions in *AtMRP1* (At1g30400), *2* (At2g34660) and *12* (At1g30410) were identified in Arabidopsis lines generated by Campisi et al. (1999) (*atmrp2-1* in Col-6/*gla1*), Forsthoefel et al. (1992) (*atmrp1-1* in Ws-2) and Bechtold et al. (1993) (*atmrp12-1* in Ws-4), and confirmed by sequencing of isolated PCR products, obtained from combinations of gene-specific and T-DNA border primers as described previously by Gaedeke et al. (2001). Individual knockout lines were subsequently isolated by scoring DNA pools representing 100 and 20 single T-DNA lines followed by PCR analysis of a population of 400 single plants corresponding to positively scored DNA pools representing 20 individual lines. Homozygous plants were identified by PCR amplification with a combination of gene-specific and T-DNA primers; heterozygous plants yielded additional PCR products with a combination of two gene-specific primers encompassing the respective T-DNA insertion (Supplementary Table I). Southern blot analyses were performed with T-DNA-specific as well as *AtMRP*-specific DNA probes for *atmrp1-1* and *atmrp2-1*. Segregation of T-DNA insertions was ascertained by crossing homozygous *atmrp1-1* and *atmrp2-1* mutant plants with the corresponding wild types. Segregation analysis of F_2 progeny revealed a 3:1 ratio for the dominant selection marker kanamycin. Co-segregation was shown by proving PCR fragment amplification with combinations of gene-specific and T-DNA border primers only with DNAs from T-DNA-containing plants. Offspring of homozygous *atmrp1-1* and *atmrp2-1* lines segregated in the F_3 generation as 100% resistant plants, while hemizygous plants segregated again in a 3:1 ratio.

Further T-DNA mutants in clade I *AtMRP* genes including *AtMRP11* (At1g30420) were identified with the help of the SIGnAL 'T-DNA Express' Arabidopsis Gene Mapping Tool (http://signal.salk.edu/cgi-bin/tdnaexpress), and seeds donated by the Salk Institute Genomic Analysis Laboratory (Alonso et al. 2003) were obtained from the NASC. The verification of the position of the T-DNA and genotyping of homozygous lines by PCR was performed essentially as described above for the mutants obtained by reverse genetic screening using primer combinations listed in Supplementary Table I.

Transcript levels of AtMRPs

RNA isolation, cDNA synthesis and PCR conditions for RT–PCR followed published procedures (Kolukisaoglu et al. 2002, Bovet et al. 2003) using the gene-specific primers indicated in Supplementary Table I. Transcripts specific for *AtMRP* genes and the 40S ribosomal protein S16 (accession No. F19995) were detected by PCR for 30 cycles at 55°C annealing temperature. Semi-quantitative RT–PCR with 0.5 MBq of [α-^{33}P]dATP (110 TBq mmol^{-1}) in the PCR mixture was performed according to Bovet et al. (2003) using 22 cycles which were in the exponential range of the PCR as determined in pilot experiments.

Promoter–GUS fusion and GUS expression analysis

As demonstrated already for *AtMRP4* (Klein et al. 2004), membrane fixation of the GUS protein using a transmembrane helix results in a less diffuse cellular GUS pattern. Therefore, the GUS protein was transcriptionally fused to the *AtMRP1* and *AtMRP2* promoter region including the first 67 and 66 amino acids of AtMRP1 and 2, respectively, which positions the GUS protein in the cytosolic loop behind the first transmembrane helix. In order to allow conformational flexibility, two glycine codons were spaced in between the truncated MRP proteins and GUS. The entire DNA fragments fused to the *uidA* gene therefore covered nucleotide

positions –2,540 to +201 and –2,627 to +198 relative to the start codon for *AtMRP1* and *AtMRP2*, respectively, and were amplified by PCR using genomic Ws-2 DNA as a template and the Herculase Enhanced DNA Polymerase Kit (Stratagene). The primers used were Pro1_upper (5′-GATC**GTCGAC**GGTCTCCTCCTCCATTA TTGGTTTACCG-3′), Pro1_lower (5′-AGTC**AGATCT**ACCAT*A CCTCC*GCAGAACTTATCCACTTTGTGATCCTTCG-3′) and Pro2_upper (5′- GATC**GTCGAC**GGGCCGGCCAAACAGTCA AGAATGCAGTC-3′), Pro2_lower (5′-AGTC**AGATCT**ACCAT*A CCTCC*GAACCTCTCCACCTTGTGATCCTTTAAG-3′) for the promoter region of *AtMRP1* and *AtMRP2*, respectively, where the *Sal*I and *Bgl*II restriction sites are highlighted in bold, respectively, while two glycine codons added in between the coding fragment of the *AtMRP* gene and the *uidA* gene to allow conformational flexibility are in italics. PCR products were cloned into *Sal*I–*Bgl*II in pCAMBIA1305.1 (www.cambia.org) thereby replacing the cauliflower mosaic virus 35S promoter, resulting in pC1305Pro$_{AtMRP1}$ and pC1305Pro$_{AtMRP2}$. Promoter and in-frame fusions of *uidA* were verified by sequencing. *Arabidopsis thaliana* Ws-2 plants were transformed by floral dipping using *Agrobacterium* strain GV3101 (Clough and Bent 1998). More than 25 hygromycin-resistant T_1 transformants for each promoter were transferred to soil, and T_2 seeds were recovered. By hygromycin selection, T_2 seed batches exhibiting a 3:1 hyg^R/hyg^S ratio were identified, and T_3 seeds of eight single plants per family were again tested for 100% hygromycin resistance before being used in GUS assays as described by Rashotte et al. (2001), using 1 mM 5-bromo-4-chloro-3-indolyl β-D-glucuronide cyclohexylamine salt (Biosynth, Stadd, Switzerland) as the substrate and overnight incubation at 37°C. Following clearing in 80% EtOH at 4°C, images of GUS-stained seedlings and tissues were taken using either a Nikon SMZ1500 binocular and a Nikon Coolpix (Egg, Switzerland) camera or a Leica DMR microscope equipped with a Leica DC300F charge-coupled device camera and controlled by Leica IM1000 software (Leica, Heerbrugg, Switzerland). Digital pictures were processed using Photoshop 7.0 (Adobe Systems).

Isolation of mesophyll protoplasts and vacuoles from A. thaliana leaves

For protoplast isolation, fully grown rosette leaves were placed with their carefully abraded (P500 emery paper) abaxial side on medium A (0.5 M sorbitol, 20 mM MES/KOH, pH 5.6, 1 mM CaCl$_2$) containing 0.03% (w/v) pectolyase Y-23 and 0.75% (w/v) cellulase Y-C for cell wall digestion (90 min, 30°C). The protoplasts were collected by centrifugation (200×g, 5 min) on a small cushion of osmotically stabilized Percoll pH 6 (0.5 M sorbitol, 1 mM CaCl$_2$, 20 mM MES, pH 6). Purification of protoplasts was performed by centrifugation (5 min, 200×g) in a discontinuous Percoll gradient where resuspended protoplasts (bottom) were sequentially over-layered with 1 vol. of medium B [0.4 M sorbitol, 30 mM KCl, 20 mM HEPES-KOH, pH 7.2, 1 mM dithiothreitol (DTT), 1 mg ml^{-1} bovine serum albumin (BSA)] containing 25% (v/v) osmotically stabilized Percoll pH 7 (0.5 M sorbitol, 20 mM HEPES, pH 7.2—middle phase) and about one-third volume of medium B without Percoll (upper phase). Concentrated protoplasts were recovered from the upper 0/25% Percoll interphase and lysed by adding the same volume of medium C [0.2 M sorbitol, 10% (w/v) Ficoll, 20 mM EDTA, 10 mM HEPES-KOH, pH 8, 160 μg ml^{-1} BSA, 1 mM DTT] pre-warmed to 42°C followed by ~10 min incubation at room temperature. Progression of vacuole release was continuously controlled by microscopy, and vacuoles were purified and concentrated by centrifugation (200×g, 5 min)

using a step gradient in 15 ml glass tubes as follows: lower phase, 1 vol. of lysate; middle phase, 1 vol. of a 1 : 1 mixture of medium C and medium D (0.4 M betaine, 30 mM KCl, 20 mM HEPES-KOH, pH 7.2, 1 mg ml^{-1} BSA, 1 mM DTT); and upper phase, 1/3 volume of medium D. Vacuoles were collected from the interface between the middle and upper phase and immediately used in transport experiments.

Uptake experiments with plant vacuoles

Vacuolar uptake experiments with [^{3}H]E$_2$17G and [^{3}H] LTC4 were performed as described earlier (Frangne et al. 2002) with some modifications. Unless indicated otherwise, for each time point and condition five polyethylene tubes (0.4 ml capacity) were prepared as follows: 70 μl of medium G [22% (v/v) Percoll, 0.4 M sorbitol, 30 mM KCl, 20 mM HEPES-KOH, pH 7.2, 0.12% (w/v) BSA, 1 mM DTT] containing 1 mM MgSO$_4$ (without ATP) or 6 mM MgSO$_4$ and 5 mM ATP (with ATP), and substrates (0.2 μCi of [^{3}H]E$_2$17G and 10 μM E$_2$17G or 20 nCi (1.27 nM) of [^{3}H]LTC4) and further substances as indicated were placed on the bottom of the tube. Uptake was started by adding 30 μl of vacuoles resuspended in medium D which were adjusted to contain 30% (v/v) Percoll pH 7.2 beforehand. The samples were rapidly overlaid with 200 μl of poly(dimethylsiloxane-co-methylphenylsiloxane) 550 (Aldrich, Buchs, Switzerland) and 60 μl of water. The incubation was terminated after 15 min by flotation of the vacuoles (10,000×g for 15 s). The level of radioactivity in the aqueous phase (50 μl) was determined by scintillation counting using 3 ml of scintillation cocktail (Readysafe Beckman Coulter, Inc., Fullerton, CA, USA). The vacuolar volume was determined in separate assays omitting the substrates but adding 0.2 μCi of ^{3}H$_2$O that rapidly equilibrated between the medium and the vacuolar lumen. Since no uptake could be observed in the absence of MgATP, uptake rates were calculated by subtracting the radioactivity measured in the absence of ATP from that measured in the presence of MgATP, unless stated otherwise.

Chlorophyll measurement and calculation of ethylene-induced chlorophyll degradation

Total chlorophyll was determined in 80% acetone extracts by spectrophotometric measurement of absorbances at 470, 647 and 663 nm using the equations of Lichtenthaler (1987). The number and appearance of rosette leaves were not affected by any of the T-DNA insertions in the *AtMRP* genes investigated. Rosette leaves of C$_2$H$_4$-treated and control plants were sampled individually following their developmental appearance from young to old leaves. By definition, the first, youngest leaf had a minimum of 1 cm in length when removed. Total chlorophyll was determined in each individual leaf and averaged over several plants per experimental series. In order to calculate the relative chlorophyll content in an ethylene-treated leaf as compared with the corresponding untreated leaf within the developmental leaf series, the following calculation was performed:

$$RC_X = \left(TC_{ethylene,X}/TC_{untreated,X}\right)/\left(TC_{ethylene,1}/TC_{untreated,1}\right)$$

where RC is the relative chlorophyll content of leaf X, and TC is the total chlorophyll measured in the first (subscript 1) or any other (subscript X) individual leaf.

Statistics

Statistical analyses were performed using SPSS 11.5, and graphs were produced using SIGMAPLOT version 8.02 (SPSS Inc., Chicago, IL, USA). The Mann–Whitney test was used to compare root length, chlorophyll content and activity of transport for toxicity, ethylene-induced chlorophyll degradation and uptake experiments, respectively, between the mutants and their corresponding wild type.

References

Alonso, J.M., Stepanova, A.N., Leisse, T.J., Kim, C.J., Chen, H., et al. (2003) Genome-wide insertional mutagenesis of *Arabidopsis thaliana*. *Science* 301: 653–657.

Bechtold, N., Ellis, J. and Pelletier, G. (1993) In planta Agrobacterium mediated gene transfer by infiltration of adult *Arabidopsis thaliana* plants. *Mol. Biol. Genet.* 316: 1194–1199.

Bovet, L., Eggmann, T., Meylan-Bettex, M., Polier, J., Kammer, P., Marin, E., Feller, U. and Martinoia, E. (2003) Transcript levels of *AtMRPs* after cadmium treatment: induction of AtMRP3. *Plant Cell Environ.* 26: 371–381.

Buchanan-Wollaston, V., Page, T., Harrison, E., Breeze, E., Lim, P.O., Nam, H.G., Lin, J.-F., Wu, S.-H., Swidzinski, J., Ishizaki, K. and Leaver, C.J. (2005) Comparative transcriptome analysis reveals significant differences in gene expression and signalling pathways between developmental and dark/starvation-induced senescence in Arabidopsis. *Plant J.* 42: 567–585.

Campisi, L., Yang, Y., Yi, Y., Heilig, E., Herman, B., Cassista, A.J., Allen, D.W., Xiang, H. and Jack, T. (1999) Generation of enhancer trap lines in Arabidopsis and characterization of expression patterns in the inflorescence. *Plant J.* 17: 699–707.

Clough, S.J. and Bent, A.F. (1998) Floral dip: a simplified method for Agrobacterium-mediated transformation of *Arabidopsis thaliana*. *Plant J.* 16: 735–743.

Cole, S.P., Bhardwaj, G., Gerlach, J.H., Mackie, J.E., Grant, C.E., Almquist, K.C., Stewart, A.J., Kurz, E.U., Duncan, A.M. and Deeley, R.G. (1992) Overexpression of a transporter gene in a multidrug-resistant human lung cancer cell line. *Science* 258: 1650–1654.

Coleman, J.O.D., BlakeKalff, M.M.A. and Davies, T.G.E. (1997) Detoxification of xenobiotics by plants: chemical modification and vacuolar compartmentation. *Trends Plant Sci.* 2: 144–151.

Dean, J.V. and Mills, J.D. (2004) Uptake of salicylic acid 2-*O*-β-D-glucose into soybean tonoplast vesicles by an ATP-binding cassette transporter-type mechanism. *Physiol. Plant.* 120: 603–612.

Edwards, R. (1996) Characterisation of glutathione transferases and glutathione peroxidases in pea (Pisum sativum). *Physiol. Plant.* 98: 594–604.

Forsthoefel, N.R., Wu, Y., Schulz, B., Bennett, M.J. and Feldmann, K.A. (1992) T-DNA insetion mutagenesis in Arabidopsis: prospects and perspectives. *Aust. J. Plant Physiol.* 19: 353–366.

Frangne, N., Eggmann, T., Koblischke, C., Weissenböck, G., Martinoia, E. and Klein, M. (2002) Flavone glucoside uptake into barley mesophyll and Arabidopsis cell culture vacuoles. Energization occurs by H^+-antiport and ATP-binding cassette-type mechanisms. *Plant Physiol.* 128: 726–733.

Frelet, A. and Klein, M. (2006) Insight in eukaryotic ABC transporter function by mutation analysis. *FEBS Lett.* 580: 1064–1084.

Gaedeke, N., Klein, M., Kolukisaoglu, U., Forestier, C., Müller, A., et al. (2001) The Arabidopsis thaliana ABC transporter AtMRP5 controls root development and stomata movement. *EMBO J.* 20: 1875–1887.

Geisler, M., Girin, M., Brandt, S., Vincenzetti, V., Plaza, S., et al. (2004) Arabidopsis immunophilin-like TWD1 functionally interacts with vacuolar ABC transporters. *Mol. Biol. Cell* 15: 3393–3405.

Henikoff, S., Greene, E.A., Pietrokovski, S., Bork, P., Attwood, T.K. and Hood, L. (1997) Gene families: the taxonomy of protein paralogs and chimeras. *Science* 278: 609–614.

Hinder, B., Schellenberg, M., Rodon, S., Ginsburg, S., Vogt, E., Martinoia, E., Matile, P. and Hörtensteiner, S. (1996) How plants dispose of chlorophyll catabolites—directly energized uptake of tetrapyrrolic breakdown products into isolated vacuoles. *J. Biol. Chem.* 271: 27233–27236.

Jasinski, M., Ducos, E., Martinoia, E. and Boutry, M. (2003) The ATP-binding cassette transporters: structure, function, and gene family comparison between rice and Arabidopsis. *Plant Physiol.* 131: 1169–1177.

Klein, M., Burla, B. and Martinoia, E. (2006) The multidrug resistance-associated protein (MRP/ABCC) subfamily of ATP-binding cassette transporters in plants. *FEBS Lett.* 580: 1112–1122.

Klein, M., Geisler, M., Suh, S.J., Kolukisaoglu, H.U., Azevedo, L., Plaza, S., Curtis, M.D., Richter, A., Weder, B., Schulz, B. and Martinoia, E. (2004) Disruption of *AtMRP4*, a guard cell plasma membrane ABCC-type ABC transporter, leads to deregulation of stomatal opening and increased drought susceptibility. *Plant J.* 39: 219–236.

Klein, M., Mamnun, Y.M., Eggmann, T., Schuller, C., Wolfger, H., Martinoia, E. and Kuchler, K. (2002) The ATP-binding cassette (ABC) transporter Bpt1p mediates vacuolar sequestration of glutathione conjugates in yeast. *FEBS Lett.* 520: 63–67.

Klein, M., Martinoia, E., Hoffmann-Thoma, G. and Weissenböck, G. (2000) A membrane-potential dependent ABC-like transporter mediates the vacuolar uptake of rye flavone glucuronides: regulation of glucuronide uptake by glutathione and its conjugates. *Plant J.* 21: 289–304.

Klein, M., Martinoia, E. and Weissenböck, G. (1998) Directly energized uptake of β-estradiol 17-(β-ᴅ-glucuronide) in plant vacuoles is strongly stimulated by glutathione conjugates. *J. Biol. Chem.* 273: 262–270.

Kolukisaoglu, H.U., Bovet, L., Klein, M., Eggmann, T., Geisler, M., Wanke, D., Martinoia, E. and Schulz, B. (2002) Family business: the multidrug-resistance related protein (MRP) ABC transporter genes in Arabidopsis thaliana. *Planta* 216: 107–119.

König, J., Nies, A.T., Cui, Y., Leier, I. and Keppler, D. (1999) Conjugate export pumps of the multidrug resistance protein (MRP) family: localization, substrate specificity, and MRP2-mediated drug resistance. *Biochim. Biophys. Acta.* 1461: 377–394.

Kreuz, K., Tommasini, R. and Martinoia, E. (1996) Old enzymes for a new job—herbicide detoxification in plants. *Plant Physiol.* 111: 349–353.

Leier, I., Jedlitschky, G., Buchholz, U., Cole, S.P., Deeley, R.G. and Keppler, D. (1994) The MRP gene encodes an ATP-dependent export pump for leukotriene C4 and structurally related conjugates. *J. Biol. Chem.* 269: 27807–27810.

Leslie, E.M., Deeley, R.G. and Cole, S.P.C. (2005) Multidrug resistance proteins: role of P-glycoprotein, MRP1, MRP2, and BCRP (ABCG2) in tissue defense. *Toxicol. Appl. Pharmacol.* 204: 216–237.

Li, Z.S., Lu, Y.P., Zhen, R.G., Szczypka, M., Thiele, D.J. and Rea, P.A. (1997) A new pathway for vacuolar cadmium sequestration in *Saccharomyces cerevisiae*: YCF1-catalyzed transport of bis(glutathionato)cadmium. *Proc. Natl Acad. Sci. USA* 94: 42–47.

Li, Z.S., Szczypka, M., Lu, Y.P., Thiele, D.J. and Rea, P.A. (1996) The yeast cadmium factor protein (YCF1) is a vacuolar glutathione S-conjugate pump. *J. Biol. Chem.* 271: 6509–6517.

Lichtenthaler, H.K. (1987) Chlorophyll and carotenoids: pigments of photosynthetic biomembranes. *Methods Enzymol.* 148: 331–382.

Liu, G., Sanchez-Fernandez, R., Li, Z.S. and Rea, P.A. (2001) Enhanced multispecificity of Arabidopsis vacuolar multidrug resistance-associated protein-type ATP-binding cassette transporter, AtMRP2. *J. Biol. Chem.* 276: 8648–8656.

Lu, Y.P., Li, Z.S., Drozdowicz, Y.M., Hörtensteiner, S., Martinoia, E. and Rea, P.A. (1998) AtMRP2, an Arabidopsis ATP binding cassette transporter able to transport glutathione S-conjugates and chlorophyll catabolites: functional comparisons with AtMRP1. *Plant Cell* 10: 267–282.

Lu, Y.P., Li, Z.S. and Rea, P.A. (1997) *AtMRP1* gene of Arabidopsis encodes a glutathione S-conjugate pump: isolation and functional definition of a plant ATP-binding cassette transporter gene. *Proc. Natl Acad. Sci. USA* 94: 8243–8248.

Martinoia, E., Grill, E., Tommasini, R., Kreuz, K. and Amrhein, N. (1993) ATP-dependent glutathione S-conjugate export pump in the vacuolar membrane of plants. *Nature* 364: 247–249.

Murashige, T. and Skoog, F. (1962) A revised method for rapid growth and bioassays with tobacco tissue cultures. *Physiol. Plant.* 15: 473–497.

Obayashi, T., Kinoshita, K., Nakai, K., Shibaoka, M., Hayashi, S., Saeki, M., Shibata, D., Saito, K. and Ohta, H. (2007) ATTED-II: a database of co-expressed genes and cis elements for identifying co-regulated gene groups in Arabidopsis. *Nucleic Acids Res.* 35: D863–869.

Rashotte, A.M., DeLong, A. and Muday, G.K. (2001) Genetic and chemical reductions in protein phosphatase activity alter auxin transport, gravity response, and lateral root growth. *Plant Cell* 13: 1683–1697.

Rea, P.A. (2007) Plant ATP-binding cassette transporters. *Annu. Rev. Plant Biol.* 58: 347–375.

Rea, P.A., Li, Z.S., Lu, Y.P., Drozdowicz, Y.M. and Martinoia, E. (1998) From vacuolar GS-X pumps to multispecific ABC transporters. *Annu. Rev. Plant Physiol. Plant Mol. Biol.* 49: 727–760.

Sakai, K., Shitan, N., Sato, F., Ueda, K. and Yazaki, K. (2002) Characterization of berberine transport into *Coptis japonica* cells and the involvement of ABC protein. *J. Exp. Bot.* 53: 1879–1886.

Sanchez-Fernandez, R., Davies, T.G.E., Coleman, J.O.D. and Rea, P.A. (2001) The *Arabidopsis thaliana* ABC protein superfamily, a complete inventory. *J. Biol. Chem.* 276: 30231–30244.

Sharma, K.G., Mason, D.L., Liu, G., Rea, P.A., Bachhawat, A.K. and Michaelis, S. (2002) Localization, regulation, and substrate transport properties of Bpt1p, a *Saccharomyces cerevisiae* MRP-type ABC transporter. *Eukaryot. Cell* 1: 391–400.

Shitan, N., Bazin, I., Dan, K., Obata, K., Kigawa, K., Ueda, K., Sato, F., Forestier, C. and Yazaki, K. (2003) Involvement of CjMDR1, a plant multidrug-resistance-type ATP-binding cassette protein, in alkaloid transport in *Coptis japonica*. *Proc. Natl Acad. Sci. USA* 100: 751–756.

Szczypka, M.S., Wemmie, J.A., Moye-Rowley, W.S. and Thiele, D.J. (1994) A yeast metal resistance protein similar to human cystic fibrosis transmembrane conductance regulator (CFTR) and multidrug resistance-associated protein. *J. Biol. Chem.* 269: 22853–22857.

Tommasini, R., Evers, R., Vogt, E., Mornet, C., Zaman, G.J.R., Schinkel, A.H., Borst, P. and Martinoia, E. (1996) The human multidrug resistance-associated protein functionally complements the yeast cadmium resistance factor 1. *Proc. Natl Acad. Sci. USA* 93: 6743–6748.

Tommasini, R., Vogt, E., Fromenteau, M., Hortensteiner, S., Matile, P., Amrhein, N. and Martinoia, E. (1998) An ABC-transporter of *Arabidopsis thaliana* has both glutathione-conjugate and chlorophyll catabolite transport activity. *Plant J.* 13: 773–780.

Zimmermann, P., Hirsch-Hoffmann, M., Hennig, L. and Gruissem, W. (2004) GENEVESTIGATOR. Arabidopsis microarray database and analysis toolbox. *Plant Physiol.* 136: 2621–2632.